

Spatiotemporal dynamics of aboveground biomass in a managed forest, central Mexico

Bossuet Gastón Cortés-Sánchez^{1*}, Gregorio Ángeles-Pérez^{1*},
Héctor Manuel de los Santos-Posadas¹, José René Valdez-Lazalde¹,
María de los Ángeles Soriano-Luna²

¹Colegio de Postgraduados, Campus Montecillo, Posgrado en Ciencias Forestales, Texcoco, Estado de Mexico, Mexico
²Comisión Nacional Forestal. Gerencia Técnica del Sistema de Monitoreo, Reporte y Verificación. Zapopan, Jalisco, Mexico

FOREST MANAGEMENT

ABSTRACT

Background: Quantifying aboveground biomass (AGB) is crucial for studying the carbon cycle and estimating mitigation potential of climate change. Combining field inventory data and remote sensing such as Landsat imagery, is a common approach for landscape-Level AGB analysis. However, uncertainties in biomass estimations persist, highlighting the need for improved statistical methods. The objectives of this study were (i) model the AGB of temperate forests managed for timber production using Landsat 8 data and three regression algorithms (linear regression, generalized additive models [GAM], and random forests), and (ii) quantify interannual AGB variations (2013–2022) across a forest landscape. Predictor variables included spectral bands, vegetation indices (VI), textural metrics, and stand age.

Results: The RF algorithm showed the best performance with accurate estimates, explaining 76% of the AGB variability. It also showed an RMSE of 32.93 Mg ha⁻¹ when stand age was included as a predictor variable. The AGB showed a spatial variation from 9 to 289 Mg ha⁻¹, and an inventory of 113,408.81 Mg (±11,663.13 Mg) in a landscape of 823.6 ha, ranging from 101,904.70 Mg in 2013 to 127,915.60 Mg in 2022. The 10-12-year-old stands showed the highest increment of biomass after a decade, increasing from 71.06 Mg ha⁻¹ (±19.81) in 2013 to 153.37 Mg ha⁻¹ (±14.13) in 2022.

Conclusion: The study evaluated a practical methodology to estimate the spatiotemporal variation of AGB in managed temperate forests. This approach can be implemented to support the evaluation of the potential contribution of managed forests to climate change mitigation.

Keywords: Landsat 8; textural metrics; vegetation indices; forest monitoring.

HIGHLIGHTS

Decade-long analysis of biomass dynamics using field data.
Random Forest regression excels in estimating aboveground biomass.
Study reveals detailed biomass variability in central Mexico forests.
Forest management enhances biomass, matching natural forest levels.

CORTÉS-SÁNCHEZ, B. G.; ÁNGELES-PÉREZ, G.; DE LOS SANTOS-POSADAS, H. M.; VALDEZ-LAZALDE, J. R.; SORIANO-LUNA, M. D. L. A. Spatiotemporal dynamics of aboveground biomass in a managed forest, Central Mexico. CERNE, v.31, e-103462, 2025. doi: 10.1590/01047760202531013462.

*Corresponding author: gangeles@colpos.mx
Scientific Editor: Luciano Cavalcante de Jesus França

Received: August 6/2024
Accepted: February 7/2025

INTRODUCTION

The world's forests play a fundamental role in the global carbon balance (Monárrez-González *et al.*, 2018). They are considered potential climate change mitigators due to their ability to store carbon (C) in plant tissue through the process of carbon dioxide (CO₂) fixation that occurs in photosynthesis. However, forests can also function as a greenhouse gas (GHG) source through their biological degradation and consequential emissions of CO₂ into the atmosphere. Natural and anthropogenic disturbances, such as forest harvesting, also cause the release of CO₂ from forests. Therefore, it is important to recognize the spatiotemporal dynamics of forest carbon reservoirs as a consequence of silvicultural interventions in addition to natural disturbance (Beer *et al.*, 2010, Köhl *et al.*, 2020).

Most of the studies that address the spatiotemporal dynamics of carbon pools in natural ecosystems have focused on unmanaged forests (Liao *et al.*, 2022, Urbazaev *et al.*, 2016). This study seeks to contribute to the knowledge of the C dynamics in managed forests for timber production because approximately 33% of the world's forests are used for this purpose (FAO, 2020) and there is uncertainty regarding the balance of emission/removal potential of GHG.

Mexico has a wide variety of forest ecosystems due to its geographic location and topographic heterogeneity. Forests in Mexico are important for their current and potentially increasing accumulation of C in their biomass (Torres-Rojo *et al.*, 2016). However, there is a lack of information on the spatial variability of AGB and the determinants that affect it, especially in managed forests (11% of the total forest area in Mexico). Temperate and tropical forests cover 64.2 million hectares, and around 10% have authorization for timber forest management (SEMARNAT, 2021). This managed forest area could be currently reducing carbon reservoirs (by degradation) or increasing C storage in the long term (new forest biomass). The precise answer to this question can only be approximated through a detailed study by ecosystem type, which will lead to decision-making regarding the most appropriate actions to maintain and improve C stores in forest ecosystems, as a complementary objective for the reduction of GHG emissions (Dugan *et al.*, 2018), while producing products for human consumption. Part of the national and global forest product consumption is obtained by applying intensive silviculture methods based on the establishment of even-aged stands (Carrillo Anzuers *et al.*, 2017, Pérez-López *et al.*, 2020).

One way to evaluate the effect of forest management is through the monitoring of C reserves, as an indicator in the context of climate change mitigation and the concept of forest degradation (Vásquez-Grandón *et al.*, 2018). This implies a comparison of C stocks at a given moment with a reference condition. Unfortunately, there is scarce information on the biomass and forest C stocks before a disturbance (Morales-Barquero *et al.*, 2014). The most common alternatives to implement this type of monitoring are through repeated field inventories

or historical information derived from measurements, although recent approaches are based on parameterization models with field information, as well as a combination of traditional inventories and remote sensing derived information (Capolupo *et al.*, 2020, Romero-Sanchez and Ponce-Hernandez, 2017). The latter enhances the ability to estimate the spatial variability of forest biomass and C content at the regional level in an explicit manner (Li *et al.*, 2019, Lu *et al.*, 2016, Macedo *et al.*, 2018). Most of the current efforts to improve the spatial estimation of biomass in several ecosystems are carried out in a single year, which does not permit the analyses of spatiotemporal dynamics of biomass and C.

The Landsat Missions consist of Earth-observing operational satellites equipped with remote sensors that have been collecting data and imagery since 1972. Landsat data have proven effective for mapping and monitoring land cover, as well as assessing land surface biophysical and geophysical properties (Wulder *et al.*, 2012). They also hold significant potential for applications in terrestrial observation, biogeochemical cycling, and land-use forecasting. Landsat data support both scientific discovery and practical uses, including resource management, environmental quality monitoring, public health, human well-being, and national security (Roy *et al.*, 2014).

At a global level, some studies analyze the multi-annual dynamics of biomass. Recently Liao *et al.* (2022) used data from Landsat sensor as variables to explain the variability of biomass at a regional scale in Australia with an acceptable precision (R² of 0.60 and RMSE of 73.1 Mg ha⁻¹) and good cost-benefit ratio and temporality of the study. They used RF to build the AGB estimation models based on the "TreeBagger" function in MatLab, relying on optical spectral reflectance. Zhu *et al.* (2022) studied the rate of biomass accumulation with data from Landsat images and an unmanned aerial vehicle in China's Fujian region, by monitoring forest parameters (canopy height) and vegetation indices (R² from 0.13 to 0.57), the annual AGB was estimated using annual Landsat EVI vegetation index maps, which were used to estimate the linear relationship between canopy height-EVI. Subsequently, the AGB was derived from the AGB-canopy height relationship. These authors argued that the choice of a type of remote sensor, and the combined use of them, represents a balance between the precision and the scale of the analysis, as well as the cost-benefit and the temporality of the findings. In Mexico, there have been no reported studies on the dynamics of AGB for a decade and the evaluation of the effect of forest management (spatial and interannual) on landscape biomass and C. In this study, we used three types of models to characterize the spatial variability of AGB in managed forests in central Mexico. The study aimed to: (i) model the AGB of temperate forests managed for timber production using Landsat 8 data and three regression algorithms (linear regression, generalized additive models [GAM], and random forests), and (ii) spatially quantify interannual variations in AGB across the forested landscape of the Intensive Carbon Monitoring Site Atopixco for the period from 2013 to 2022.

MATERIAL AND METHODS

Study Site

The study site is located in the Zacualtipán - Molango forest region, in the state of Hidalgo, central Mexico; between the geographical coordinates 20°40'17" and 20°34'51" N, 98°40'07" and 98°34'22" W, at an altitude of 2000 m.a.s.l. It is a mountainous landscape with the presence of pine-oak and tropical mountain cloud forests (Ángeles-Pérez et al., 2015). It shows a temperate-humid climate with a mean annual temperature of 14.4 °C, rains from June to October, and a rainfall of 1325.8 mm (SMN, 2020).

The study site covers a polygon of 900 ha landscape that corresponds to the Intensive Carbon Monitoring Site Atopixco (ICMS Atopixco) (Ángeles-Pérez et al., 2015). It is dominated by even-aged stands regenerated through the Silvicultural Development Method (MDS in Spanish), implemented in the early 1980s. The dominant species is *Pinus patula* Schiede ex Schltdl. & Cham., mixed with other species such as *P. teocote* Schiede ex Schltdl, several species of *Quercus* spp, and other broadleaved species. Thirty percent of the area is covered by stands over 90 years of age that have never been silviculturally intervened, which are considered 'natural' (Soriano-Luna et al., 2018).

The ICMS Atopixco was established in 2012, to develop and implement methods for the evaluation and monitoring of forest carbon in managed forests for timber production (Ángeles-Pérez et al., 2015) (Figure 1).

Field Information

In 2013, 40 primary sampling units were established according to the plot design of the National Forest and Soil Inventory of Mexico (CONAFOR, 2012). Each primary sampling unit is settled by 4 secondary sampling subunits, 400 m² each, arranged in an inverted "Y" shape. In all sampling units, the diameter at breast height (*dn*) and total height (*at*) of all trees (*dn* ≥ 5 cm) were measured. The individual volume (*vta* in m³) and biomass (*B* in kg) were calculated with models developed by Soriano-Luna et al. (2015). We identified 31 management units with different ages in the landscape, considering from the time elapsed since harvesting. Remeasurements were carried out in 2014, 2016, and 2019. In addition, the number of individuals per hectare (N ha⁻¹) and the basal area per hectare (m² ha⁻¹) were determined using the following expression:

$$AB = \left(\frac{\pi}{40000} \times dn^2 \right)$$

Remote Sensing Information

Images from the Landsat 8 platform were used (route/rows: 026/036, cloud cover <10%), one for each year of the period 2013 to 2022. The images have a spatial resolution of 30×30 m, level 1 processing with reflectance calibrated at

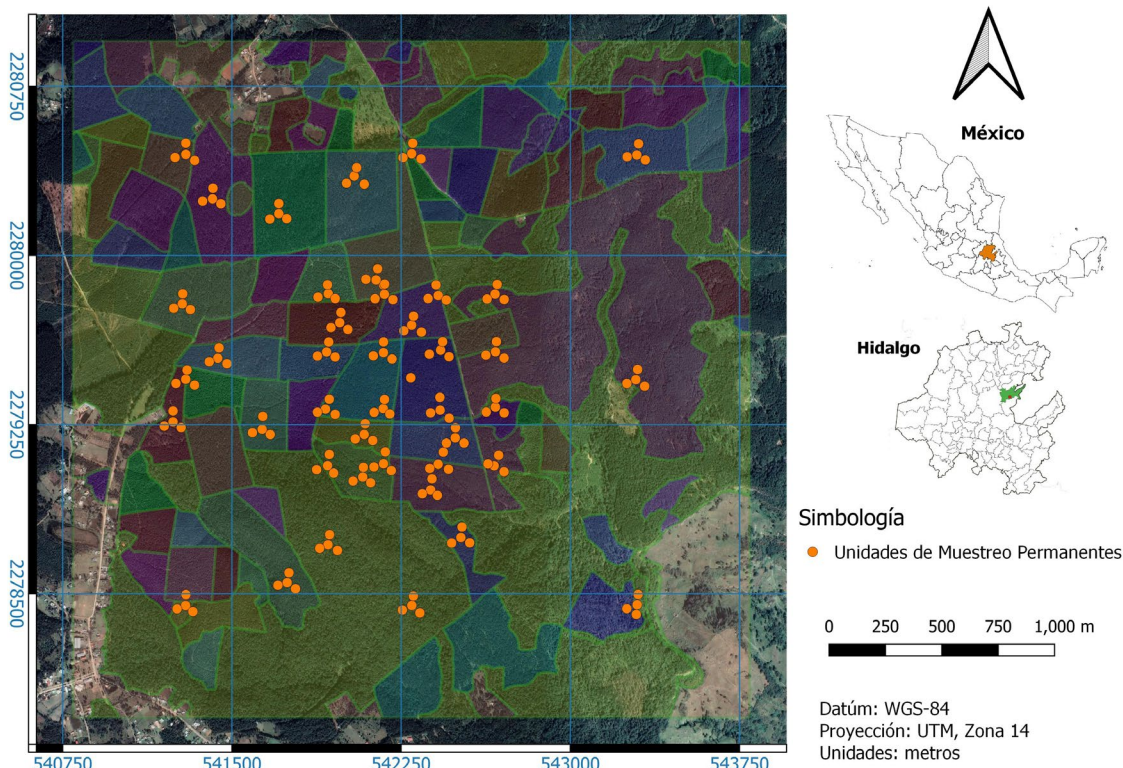


Figure 1: Study site location and permanent sampling plots at Intensive Carbon Monitoring Site Atopixco.

the top of the atmosphere (TOA). The information for their calibration was extracted from the image metadata (Chander *et al.*, 2009). The spectral values of five bands were used: blue, green, red, infrared, and shortwave infrared. The mean of the band values in the dry season was used to represent the bands annually, to reduce conflict due to atmospheric variations, generating an image for each year of the study period (2013 to 2022). The control procedures were carried out using the *Google Earth Engine* platform (Zhu *et al.*, 2022). All images were normalized in the *R* software with the *histMatch* function of the *RStoolbox* package (Goslee, 2011, Leutner *et al.*, 2019). The normalized difference vegetation index (NDVI) and its variants were calculated (Table 1) (Aguirre-Salado *et al.*, 2012, Sader *et al.*, 1989): the soil-adjusted vegetation index (SAVI), the enhanced vegetation index (EVI) (Macedo *et al.*, 2018, She *et al.*, 2015), the advanced vegetation index (AVI) and Simple Ratio (Li *et al.*, 2020, Silleos *et al.*, 2006). Additionally, eight spectral texture metrics were generated; mean, variance, homogeneity, contrast, dissimilarity, entropy, second moment, and correlation for the five bands and the VIs using the *GLCM* library of the *R* software (Zvoleff, 2020). Therefore, from the five bands and seven vegetation indices, eight textural metrics were generated. We created a dataset with 108 spectral variables derived from Landsat 8 images. These variables were used as initial predictors in the fit process of aboveground forest biomass models. Specifically, the dataset included spectral values of the bands, vegetation indices, and textural metrics based on the gray-level co-occurrence matrix (Table 1) (Zvoleff, 2020).

The extraction of spectral values of the images is performed based on the coordinates of the center of the

secondary sampling plots established in the field, extracting the value of each pixel. These data were used as the values for each sampling unit according to the methodology proposed by Hernández-Stefanoni *et al.* (2021a).

Algorithms and Model Fitting

The biomass calculated from field data for each permanent sampling unit was used as a response variable, while the information from Landsat images was used as predictor variables (Table 1). We developed several kinds of models to fit our data for predicting the AGB (Mg ha⁻¹) across the landscape (spatial variability of AGB) from the set of predictor variables. The data from the images corresponding to the year of field measurements were used to fit generic linear regression (LM), generalized additive (GAM) and Random Forest (RF) models. Further, we estimate the AGB per year for a decade.

The linear model (LM) was used as a reference to evaluate the association between the response variable and the dataset of explanatory/predictor variables and identify highly-correlated variables and determine the best-fit. In order to find a model with the greatest explanatory power. Multiple regressions are often affected by overfitting and collinearity among variables. Since it is common to find multicollinearity when using the band reflectance, vegetation indices, as well as textures (Zhang *et al.*, 2015), the variance inflation factor (VIF) was used to evaluate it and remove highly correlated variables from the model (Li *et al.*, 2019). Considering a possible non-linear relationship between AGB and the metrics derived from Landsat 8, the Generalized

Table 1: Variables derived from Landsat 8, vegetation indices and textures, used to estimate aboveground biomass.

Type	Name	Number	Description
Band reflectance	Blue band (B2)	5	Landsat 8 band reflectance
	Green band (B3)		
	Red band (B4)		
	Near infrared (B5)		
	Shortwave infrared 1 band (B6)		
Vegetation indices (VI)	NDVI	7	Normalized difference vegetation index
	NDVI ₅₃		NDVI (<i>infrared</i> – <i>green</i> / <i>green</i> + <i>infrared</i>)
	NDVI ₆₅		NDVI (<i>SWIR1</i> – <i>infrared</i> / <i>SWIR1</i> + <i>infrared</i>)
	SAVI		Soil-adjusted vegetation index
	EVI		Enhanced vegetation index
	AVI		Advanced vegetation index
	SR		Simple ratio index
Textural metrics	Mean (<i>md</i>)	96	Textural metrics using gray-level co-occurrence matrix
	Variance (<i>v</i>)		
	Homogeneity (<i>h</i>)		
	Contrast (<i>con</i>)		
	Dissimilarity (<i>d</i>)		
	Entropy (<i>e</i>)		
	Second moment (<i>sm</i>)		
	Correlation (<i>cor</i>)		

Additive Model (GAM) was fitted, a semi-parametric approach (Hastie and Tibshirani, 1990), for predicting the nonlinear responses of biomass to the set of predictor variables. GAMs are regression models that generalize the family of generalized linear models (GLMs), by replacing the linear functional form by a sum of smooth functions. GAMs have been strongly accepted in several domains as a flexible modeling technique, suited for capturing nonlinear, unspecified relationships between predictor variables and the response variable. GAMs have been used to model AGB from remote sensing information (Li et al., 2020; Soriano-Luna et al., 2018). GAM regression was carried out using the R packages *mgcv* (Wood and Wood, 2015) Also, the regression model of the Random Forests (RF) algorithm was used as another prediction model. RF is a machine learning algorithm that has been shown to reduce bias and overfitting. This is based on decision trees from the random selection of variables and samples. RF has been widely used for quantitative analysis, as well as for forest cover classification and AGB estimations (Jiang et al., 2020, Zhou et al., 2021). In some cases, tends to be more accurate than simple regression techniques for biomass estimation (Li et al., 2020).

The selection of predictor variables to be included in the models to estimate AGB was carried out using the *stepwise* procedure for linear models (Olusegun et al., 2015), and for RF models with the *varimport* function from the *randomForest* library (Breiman et al., 2018); with the best model we estimate the AGB of the study area. In a second modeling phase the predictor variable "stand age" was added to evaluate its contribution to the explanation of AGB variability (Zhu et al., 2022). With the best model identified, an inference of the AGB was performed for a decade.

Model Evaluation

The three generic models were evaluated through 10-fold repeated cross-validation, where the dataset was subdivided into 10 subsamples, each model was trained on 9 of the subsamples, and tested on the remaining sample (Tyralis et al., 2019). To qualify the performance of the models, the value of the coefficient of determination (R^2), the root mean square error (RMSE), the mean absolute error (MAE), and the mean absolute percentage error (MAPE) were used (Equations 1, 2, 3 e 4). Models with higher R^2 and lower RMSE and MAE values indicate a better performance. Finally, the best predictive model was used to map the spatial distribution of AGB for the landscape using the *ModelMap* library in R software (Freeman et al., 2018).

$$R^2 = \frac{\sum_{i=1}^n (Y_p - \bar{Y})^2}{\sum_{i=1}^n (Y_o - \bar{Y})^2} \quad (1)$$

$$RMSE = \left[\frac{\sum_{i=1}^n (Y_o - Y_p)^2}{n} \right]^{0.5} \quad (2)$$

$$MAPE = \frac{100}{n} \sum_{i=1}^n \frac{|Y_o - Y_p|}{Y_o} \quad (3)$$

$$MAE = \frac{\sum_{i=1}^n |Y_p - Y_o|}{n} \quad (4)$$

Where: Y_o and Y_p are the observed and predicted biomass respectively, and n is the number of observations.

To evaluate the estimation of AGB obtained from the Landsat 8 sensor, the biomass inventory for each year was calculated with field data (2013, 2014, 2016, and 2019) and we compared results. The field inventory for each measurement year was calculated using ratio estimators incorporating auxiliary information on the basal area (BA). This approach has proven to be more reliable and precise than simple random sampling since the BA depends on the diameter at breast height, a variable with the lowest measurement error in field inventories (Roldán-Cortés et al., 2013).

Uncertainty Estimation

The best model was used to determine the spatially explicit uncertainty of the AGB estimates. We calculated the standard deviation, the coefficient of variation (CV), and the confidence interval (Ortiz-Reyes et al., 2021). For the LM and GAM models, we used confidence intervals (CI) through ± 2 standard deviations from the estimated mean (Soriano-Luna et al., 2018). For the RF model, the uncertainty was evaluated and mapped using the CV associated with estimates generated at the pixel level. This estimation was performed with the *ModelMap* package of the R software (Freeman et al., 2018).

RESULTS

Estimation of Aboveground Biomass

The three model approaches (LM, GAM, and RF) were evaluated using coefficient of determination (R^2) and root mean square error (RMSE) as metrics for evaluating goodness-of-fit. The methods LM and GAM showed a limited explanation of AGB variability (lower R^2 and higher RMSE). When stand age was included as a predictor variable, these models improved their goodness of fit statistics (Table 2). Among the three |tested models, RF2 was the one that showed the best performance to model AGB. It had an R^2 of 0.76 and an RMSE of 32.93 Mg ha⁻¹, including age as a predictor variable was possible to reduce to five the number of predictor variables derived from Landsat 8 sensor. On the other hand, the RF1 model showed a moderate performance with an R^2 of 0.43 y un RMSE of 51.26 Mg ha⁻¹ only using information derived from Landsat 8. Predictor variables were selected using the *stepwise procedure* for linear models. Including the stand age variable altered the model structure, leading to the replacement of some

variables. A similar effect was observed when using the *varimport* function from the *randomForest* library.

The MAPE and MAE statistics confirmed the fit of the proposed models (Table 2). The RF models registered the lowest RMSE values. The inclusion of stand age as a predictor variable provides an important gain to explain the variability of AGB (Figure 2). The field information indicates that the stands show a high variability of AGB during the first 10 years of age with an average of 46.38 Mg ha⁻¹ (±19.07). The stands maintain an upward trend in the accumulation of biomass until the age of 25 years, afterwards, they show a stabilized biomass content with a mean of 193.19 Mg ha⁻¹ (±38.34).

Biomass Mapping at the Landscape Level

The total AGB estimation with the RF2 model varied from 96 525.87 to 129 412.18 Mg in 823.6 ha over a decade. Spatial changes in the distribution of biomass in the forest landscape were observed during the period evaluated (Figure 3). The lower biomass values match with recent harvest areas, and therefore in younger stands.

The AGB was quantified for one decade by the RF2 model. This estimation was contrasted with that obtained through the field inventory using the Proportion (Ratio) estimation method. The annual quantification of biomass in the forest landscape was carried out by summing the values of each pixel, considering the entire landscape area (total population). As a result, the biomass estimation did not include confidence intervals. In contrast, when using the sampling technique to estimate AGB, information is collected from only a proportion of the population within the study area. Therefore, when conducting AGB inventory through sampling, it is essential to present the confidence interval, which describes the variability between the value obtained in the study and the true population value, providing a high probability of including the actual value.

In general, slightly higher biomass estimates were observed from the Landsat 8 sensor variables, being lower

than field estimates only in the 2019 measurement. The field inventory estimates overlapped within the 95% CI limits in 2013 and 2019 and were close in 2014 and 2016 (Table 3); the AGB of the forest landscape was estimated for each year evaluated with the RF1 model, greater biomass was quantified, estimating in the period 2013-2017 up to 37% more biomass, after 2019 the estimated AGB was similar for the models.

Temporal Dynamics of Aboveground Biomass by Stand Age

The dynamics of biomass accumulation over a decade in stands of different ages indicated that recently harvested stands (1-2 years old) had an average biomass of 59.59 Mg ha⁻¹ (±20.04) in 2013 and 66.58 Mg ha⁻¹ (±20.36) in 2022 (Figure 5). On the other hand, the stands of 10-12 years registered the greatest increment of biomass after a decade, increasing from 71.06 Mg ha⁻¹ (±19.81) in 2013 to 153.37 Mg ha⁻¹ (±14.13) in 2022. In stands older than 30 years (30-32) and in the unmanaged forest, the increment in biomass was relatively low (Figure 4). It is worth mentioning that between stands >30 years old and the natural forest, no statistically significant differences were observed in terms of accumulated biomass in the study period, with the only exception in the year 2018.

Spatial Uncertainty

The spatial uncertainty of biomass variability was expressed as a percentage of the coefficient of variation (CV). Maps of the CV were generated where the areas with the highest estimation errors of biomass were identified (Figure 5). Also, interannual uncertainty ranged between 0% and 50% in most of the area. However, in some areas, there was high uncertainty (>100%). These areas corresponded to open areas and young stands on the landscape. Because the uncertainty is represented in percentage, it turns out to be higher for small biomass values. Therefore, small variations in biomass result in a larger percentage variation.

Table 2: Goodness of fit of models evaluated to estimate aboveground biomass from remote sensing information.

Id	Model structure	R ²	RMSE	MAPE	MAE
LM1	$B = 480.7 - 351.9(B6md) - 1528(B2md) - 50.31(SRv) + 360.6(EVI) + 81.81(B4h) + 17.05(AVId)$	0.30	57.04	0.92	44.93
LM2	$B = 1167 + 2.115(Age) - 1084(B3md) - 726.3(NDVI53md) - 1199(B2md) + 1.61(B4v) - 12.03(SRcor)$	0.55	45.79	0.64	35.57
GAM1	$B = s(B6md) + s(B2md) + s(SRv) + s(EVI) + s(B4h) + s(AVId)$	0.30	57.40	0.84	44.55
GAM2	$B = s(Age) + s(B3md) + s(NDVI53md) + s(B2md) + s(B4v) + s(SRcor)$	0.69	37.85	0.46	28.41
RF1	$B = B4 + B3md + B4v + B6md + B6v + B6 + B4md + B2v + B3v + B3 + B2md + NDVI65md + NDVI53v + NDVI53md + SRv + B5md$	0.43	51.26	0.30	38.73
RF2	$B = Age + B3md + NDVI53md + B2md + B4v + SRcor$	0.76	32.93	0.25	23.68

Where: B2, B3, B4, B5, and B6, are reflectance of the Landsat 8 bands. NDVI53, NDVI65, SAVI, EVI, AVI, and SR; NDVI (infrared – green / green + infrared), NDVI (SWIR1 – infrared/ SWIR1 + infrared), Soil Adjusted Vegetation Index, Enhanced Vegetation Index, Advanced Vegetation Index, and Simple Ratio Index. md (Mean), v (Variance), d (Dissimilarity), and cor (Correlation); Textural metrics using gray levels from the co-occurrence matrix.

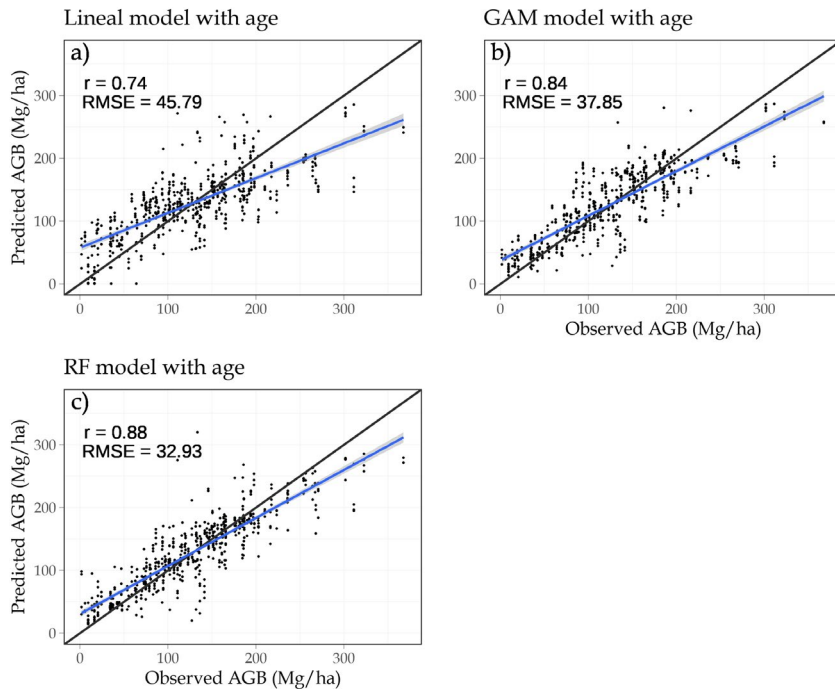


Figure 2: Relationship between aboveground biomass observed and predicted by the evaluated models. The solid line represents the 1:1 ratio. The blue line is the regression line between observed and predicted biomass.

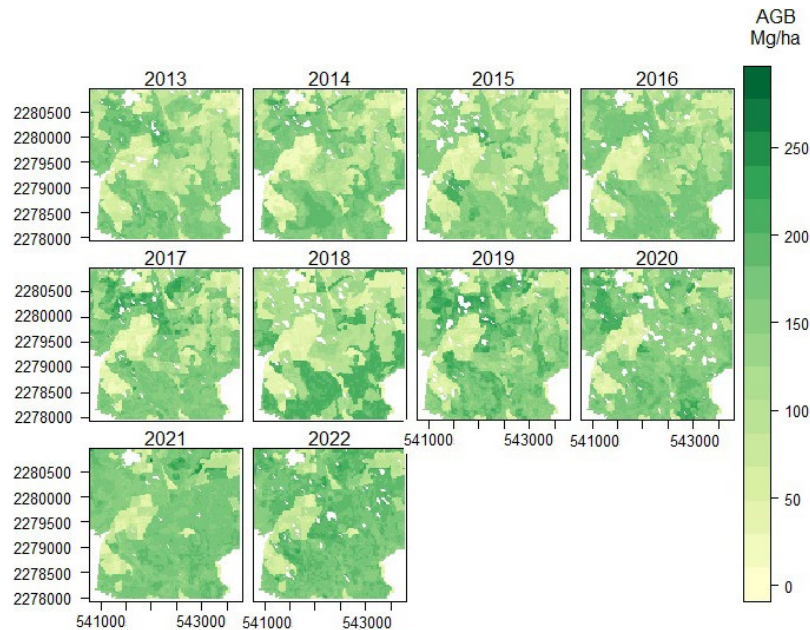


Figure 3: Spatiotemporal dynamics of the aboveground biomass distribution at the Atopixco Intensive Carbon Monitoring Site, Mexico.

DISCUSSION

Knowledge of the dynamics of forest ecosystems, especially managed forests, is essential to ensure their proper management. To understand the role of managed forests to remove and store atmospheric carbon, it is

necessary to quantify the effects of forest management actions on stored biomass and to develop comparative analyses between managed.

The parameters of goodness of fit of the LM1 and LM2 models are comparable to those reported by Li *et al.* (2019). They used linear models to predict biomass in

mixed, spruce, and coniferous forests, and obtained an R^2 between 0.10 and 0.22, and RMSE between 18.41 and 28.47 Mg ha⁻¹ from data. However, when they stratified the forest by crown density (sparse, medium, and dense), the fit estimators improved substantially ($R^2 = 0.39 - 0.61$ and RMSE = 16.05 - 23.12 Mg ha⁻¹). In our analysis, the LM2 model showed higher R^2 than the linear models. However, an improvement was obtained for the RMSE.

Table 3: Estimated aboveground biomass (Mg) using the Random Forest algorithm, with Landsat 8 and field inventory data, for the period 2013-2022.

Year	Landsat 8		Inventory	
	Total (Mg) RF1	Total (Mg) RF2	Total (Mg*)	±IC 95%
2013	120,360.51	101,904.70	96,745.30	7,537.16
2014	112,839.10	102,387.10	87,996.79	8,399.03
2015	132,324.82	96,525.87		
2016	131,937.89	106,346.87	95,372.67	8,341.79
2017	116,996.32	110,313.73		
2018	133,124.30	119,872.00		
2019	130,202.67	129,412.18	142,391.88	15,349.71
2020	120,093.02	115,326.77		
2021	123,494.66	124,083.30		
2022	117,464.18	127,915.60		

* Measurements years. CI: Confidence interval with 95% reliability.

An appropriate correlation was detected between the variables derived from textural metrics, particularly between the “mean” of the reflectance bands and vegetation indices; NDVI53, AVI, EVI, and SR, which improved the model goodness-of-fit. However, the stand age provided the highest improvement to the models, explaining up to 76% of the variability of AGB in the RF2 model.

The inclusion of information from textural metrics derived from the Landsat 8 sensor helped to explain the

variability of AGB, especially for forests with complex structures like those present in unharvested areas. These textural metrics presented abundant information to improve the performance of models for the estimation of AGB, as pointed out by Li *et al.* (2020).

When there is no information on stand age, it is possible to estimate AGB from information derived from Landsat 8. For example, it has been shown that the performance of models for uneven-aged forests or areas with moderate intensity of silvicultural treatments is improved through an adequate stratification of the forest landscape (Li *et al.*, 2019). This analysis was excluded because the study area is under intensive forest management. Nonetheless, the stands resulting from regeneration cuts showed their role in stratification. While stand age is typically treated as a numerical variable, it can also be incorporated into models as a qualitative variable.

For stands with high biomass densities, the models that do not account for stand age showed a limited ability to explain the AGB variability (Figure 3). In this regard, several studies have reported an underestimation of biomass in stands with high densities based on information from remote sensing-derived data (Hernández-Stefanoni *et al.*, 2021b, Li *et al.*, 2019, Torres-Vivar *et al.*, 2017), mainly due to problems of saturation of bands used as forest density increases (Singh *et al.*, 2023).

Overestimation and underestimation problems were experienced by all tested models in our study. However, this problem was reduced by employing standage as a predictor variable in the RF2 model. Factors such as age, density, and floristic composition directly influence the capacity of forest ecosystems to store biomass. These factors are typically altered by forest management or natural disturbances and are reflected in changes in the distribution of carbon within the ecosystem (Chavez-Aguilar *et al.*, 2022). The predicted value is higher than the 1:1 line when biomass is low (AGB ≤ 35 Mg ha⁻¹) but lower when it is high (AGB ≥ 235 Mg ha⁻¹) (Figure 3). This suggests that the models still overestimate the lowest AGB values (6.5%) and underestimate the

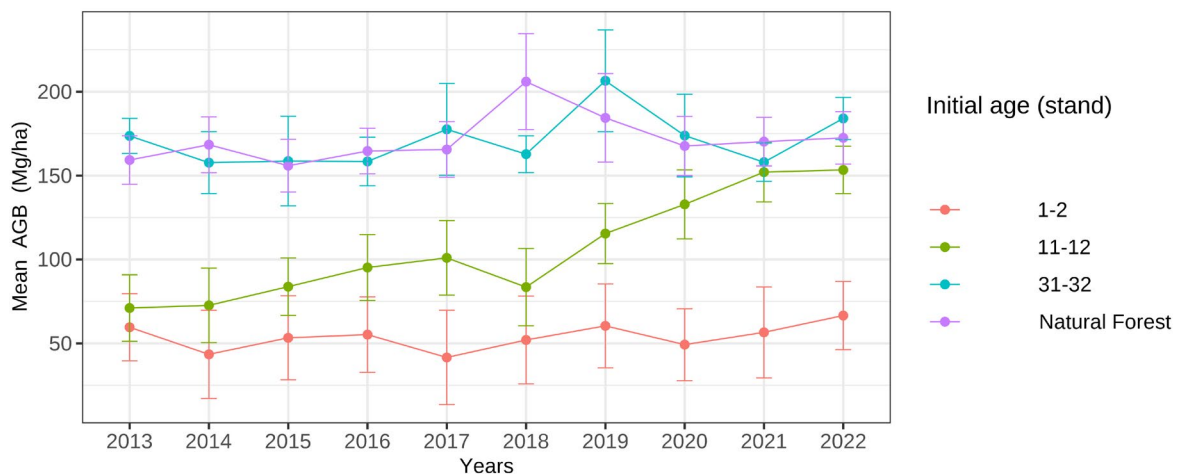


Figure 4: Biomass accumulation in stands of different ages. The initial age represents the age of the stand recorded in 2013. Natural forests are stands that have not been harvested.

highest biomass values (9.8%). Hernández-Stefanoni *et al.* (2020), Soriano-Luna *et al.* (2018) and Li *et al.* (2020) also reported this problem in biomass studies, mainly due to the high variability of information derived from Landsat 8 that it presented in young stands and the saturation of the same bands in highly dense stands.

Variables Ranking Explaining Aboveground Biomass

With the *varimport* function of the *randomForest* library, we identified 15 of 108 spectral variables with significant importance in AGB models. This indicates that a large amount of remote sensing information does not always help to explain the variability of forest parameters. The correct selection of the textural metrics had a considerable influence on the improvement of the estimation of AGB. The textural metrics referring to the mean (*md*) of bands and VI turned out to be significant in explaining the variability of AGB and other features of the studied stands. Li *et al.* (2019) reported similar results for a humid subtropical forest where they used the textural metric of the mean (*md*) of band 3 and the correlation metric (*cor*) of bands 2 and 7 of the Landsat 8 sensor. Ochoa-Franco *et al.* (2019) explored textural metrics to model forest diversity, where they used the *md* of band 4 and the variance (*v*) of band 5 based on RapidEye-derived information in a tropical semi-evergreen forest, explaining 68.5% of the spatial variability. Li *et al.* (2020) also used information from textural metrics in a humid tropical forest to estimate AGB, the *md* textural metric of band 2 and band 4 of the Landsat sensor of high

importance. Our results coincide with such studies, where the textural metric of the *md* of bands 2, 3, and the NDVI53 best explained the spatial variability of AGB.

Biomass Estimates and Uncertainty

Several studies have shown good goodness-of-fit parameters to estimate biomass on a large scale. In the state of San Luis Potosí (Mexico), MODIS sensor images with a resolution of 500 m were used to estimate AGB and it obtained RMSE values less than 27.9 Mg ha⁻¹ (Aguirre-Salado *et al.*, 2012). At the national level in Mexico, an RMSE of 36.1 Mg ha⁻¹ was obtained using MODIS and ALOS PALSAR images (Rodríguez-Veiga *et al.*, 2016). AGB estimations carried out in the same study area reported RMSE similar to those obtained in our study. For example, Torres-Vivar *et al.* (2017) reported a RMSE in AGB of 17.0 to 33.5 Mg ha⁻¹. Ortiz-Reyes *et al.* (2015) with information derived from LiDAR obtained 33.5 Mg ha⁻¹ of RMSE. Soriano-Luna *et al.* (2018) obtained the best biomass estimators for the region with an RMSE of 17.0 Mg ha⁻¹, using LiDAR sensor information. However, none of the previous studies reported a multi-year estimation or described the biomass dynamics in the landscape. In this study, we obtained an RMSE of 32.93 Mg ha⁻¹, which is similar to the previously cited studies. AGB values were estimated in a range from 9 to 289 Mg ha⁻¹. The average estimation of AGB at the pixel level for 2013 and 2014 was 125 Mg ha⁻¹, and 130 Mg ha⁻¹ in 2016 (Figure 6). For the year 2019, the algorithm reported an increment of

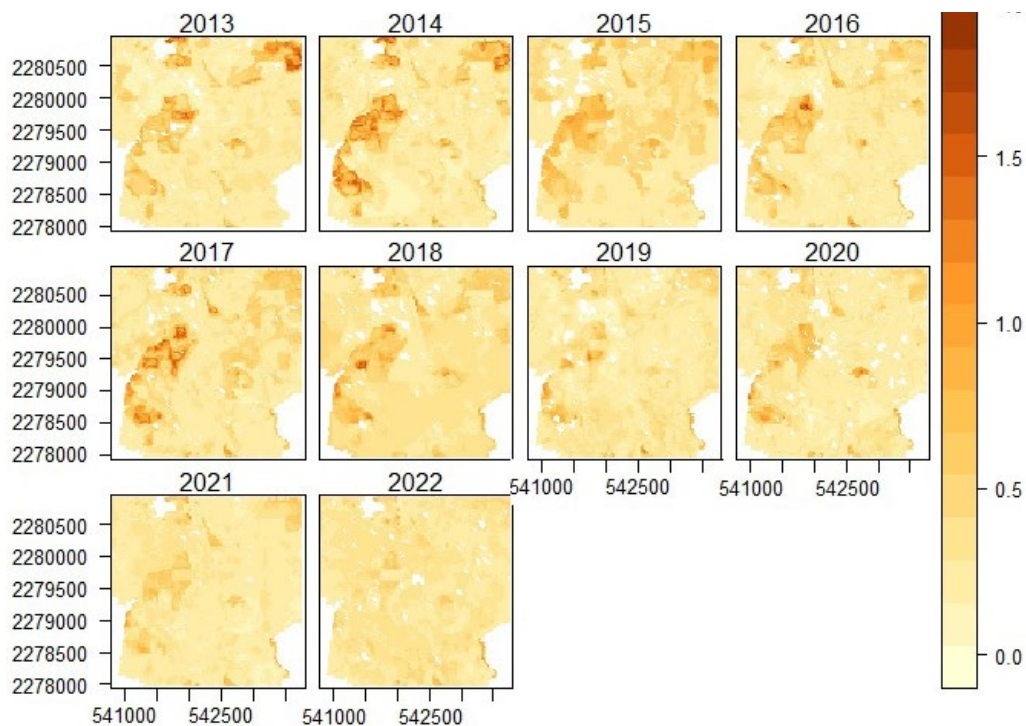


Figure 5: Spatial distribution of coefficients of variation (CV) of the estimation of aboveground biomass in the Atopixco Intensive Carbon Monitoring Site.

the average aboveground to 160 Mg ha⁻¹, similar to that estimated through field inventory (172.88 Mg ha⁻¹). This suggested that AGB in the forests for timber production increased compared to estimates in previous years.

The AGB estimates in the study area in some years were not uniformly distributed (Figure 6). Therefore, the median value may be more appropriate to describe the biomass distribution in the forest landscape. We observed an increment in the median of aboveground biomass from 2013 to 2019, from 146 Mg ha⁻¹ to 169 Mg ha⁻¹. This indicates

that the information from the Landsat 8 sensor and derived textural metrics provided estimates similar to that of previous reports with specific sensors and synergies among them (Ortiz-Reyes *et al.*, 2015, Torres-Vivar *et al.*, 2017).

The coefficient of variation (CV) has been widely used to report the spatial variation of the uncertainty of the AGB estimates. In our study, the CV values were similar to the uncertainty reported by Soriano-Luna *et al.* (2018), for the same ecosystem (mostly 0% to 100%). Also, Ortiz-Reyes *et al.* (2021) reported an uncertainty of up to 100% in

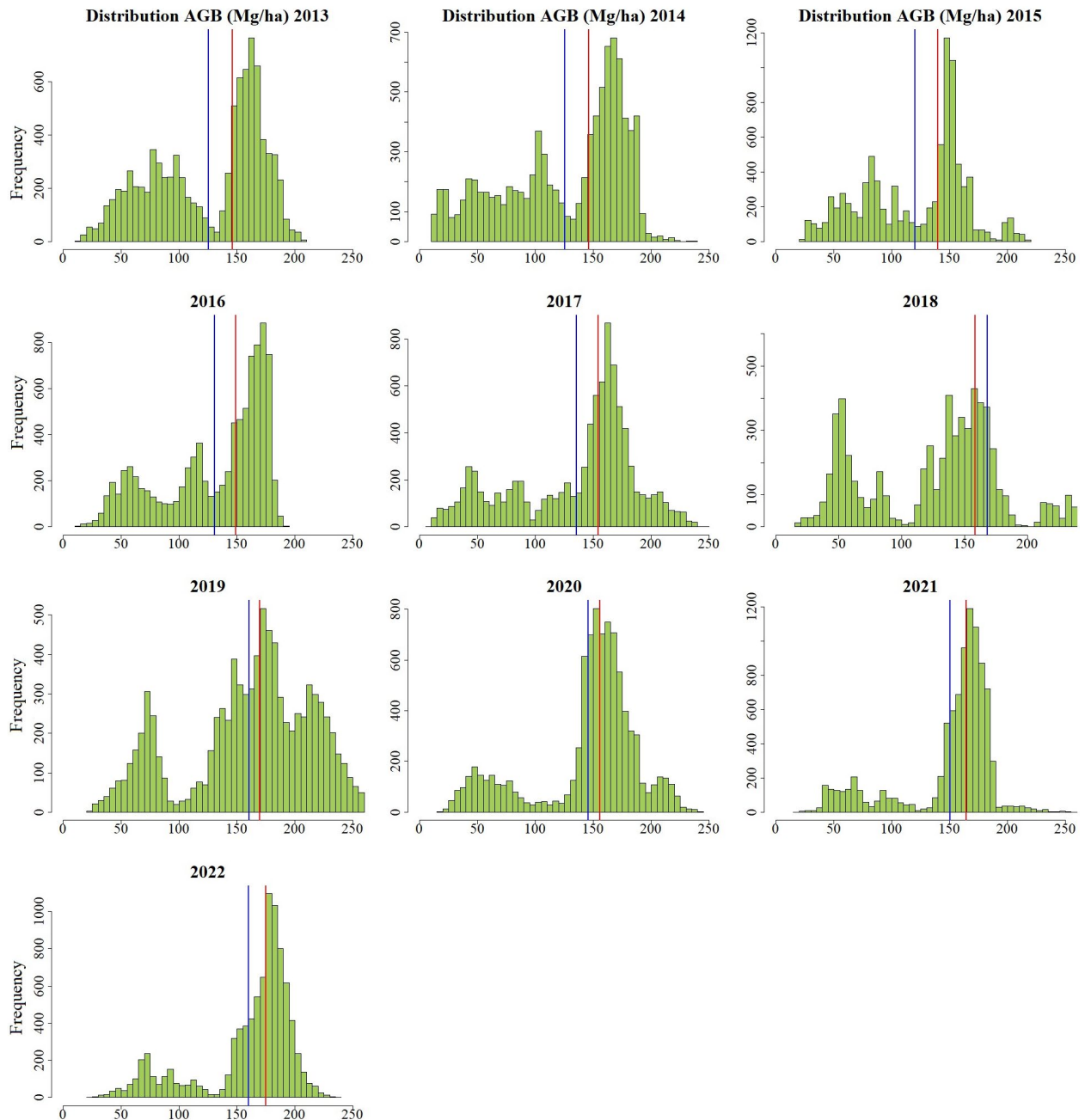


Figure 6: Aboveground biomass was predicted with the RF model where stand age was included as a predictor variable for a forested landscape in Atopixco Intensive Carbon Monitoring Site, for a decade. The blue line is the mean, while the red line represents the median of the distribution.

maps of AGB of semi-evergreen and deciduous forests. On the other hand, Hernández-Stefanoni *et al.* (2020) reported uncertainties of up to 75% in tropical forest biomass maps of the Yucatan Peninsula, Mexico. In both studies, only one year was reported, while in our study the spatial variability of AGB was analyzed throughout a decade; therefore, a higher variability was expected.

One component that could increase the uncertainty in our study was the acquisition date of the different scenes of the Landsat 8 sensor that were used. Although we applied a normalization process to make all images compatible and to reduce variation between scenes (Steinhausen *et al.*, 2018), such variation may not have been sufficiently reduced. The uncertainty could also be influenced by the interannual variability of the estimated biomass, based on information from four field measurements. The young stands presented the greatest uncertainty, while the stands older than 20 years of age showed less uncertainty, in general, the uncertainty was less than 40% in the forest landscape (Figure 5).

The estimation of AGB using satellite imagery plays an important role in climate change mitigation strategies by providing accurate in terrestrial ecosystems. It enables the estimation of the amount of stored carbon and annual variations due to growth, deforestation, or forest degradation. It also facilitates the identification and monitoring of land-use changes, helping to detect deforestation areas and assess their impact on emissions. Furthermore, it supports the implementation of programs such as REDD+ (Reducing Emissions from Deforestation and Forest Degradation), which require precise measurements of carbon reserves to calculate financial incentives associated with forest conservation. It also allows for the assessment of the impact of events such as wildfires, droughts, or human activities, providing real-time information on associated emissions.

CONCLUSIONS

The combination of field data and annual information derived from the Landsat 8 sensor made it possible to study for a decade, the dynamics of AGB of a managed forest for timber production. The developed method was appropriate for AGB estimates and mapping in multiannual periods as a complementary activity to monitoring forest resources. The Random Forest (RF) algorithm showed the best goodness-of-fit parameters. Two types of models were fitted; one that was evaluated only with information derived from the Landsat sensor provided an acceptable explanation of the spatial variability of AGB, with an $R^2 = 0.43$ and an RMSE of 51.26 Mg ha^{-1} . Nevertheless, including stand age as a predictor variable substantially improved the explanation of AGB variability of the forested landscape ($R^2 = 0.76$ and $\text{RMSE} = 32.93 \text{ Mg ha}^{-1}$). The information from the Landsat 8 sensor, as well as the textural metrics, provided AGB estimates similar to that obtained with other sensors with higher spatial resolution. However, Landsat images are freely accessible and provide a broad temporal catalog of images before current sensors. Although underestimations of high AGB values and overestimation of low values still occurred,

the RF algorithm reduced this problem. Therefore, the use of information derived from the Landsat 8 sensor can be used effectively to estimate biomass at the landscape level. This approach has significant practical implications, such as precise biomass quantification to support sustainable forest management, to identify critical areas for conservation, and it aids in reporting carbon emissions and removals to develop climate change mitigation strategies.

AUTHORSHIP CONTRIBUTION

Project Idea: B. G. C-S.; G. A-P.

Funding: G. A-P.

Database: B. G. C-S.; G. A-P.; J. R. V-L.; M. A. S-L.

Processing: B. G. C-S.; G. A-P.; H. M. S-P.; J. R. V-L.; M. A. S-L.

Analysis: B. G. C-S.; G. A-P.; H. M. S-P.

Writing: B. G. C-S.; G. A-P.

Review: B. G. C-S.; G. A-P.; H. M. S-P.; J. R. V-L.; M. A. S-L.

REFERENCES

- AGUIRRE-SALADO, C. A.; TREVIÑO-GARZA, E. J.; AGUIRRE-CALDERÓN, O. A., *et al.* Construction of aboveground biomass models with remote sensing technology in the intertropical zone in Mexico. *Journal of Geographical Sciences*, v. 22, n. 4, p.669-680, 2012.
- ÁNGELES-PÉREZ, G.; MÉNDEZ-LÓPEZ, B.; VALDEZ-LAZALDE, J. R., *et al.* Estudio de Caso del Sitio de Monitoreo Intensivo del Carbono en Hidalgo. Montecillo, México, 2015.
- BEER, C.; REICHSTEIN, M.; TOMELLERI, E., *et al.* Terrestrial Gross Carbon Dioxide Uptake: Global Distribution and Covariation with Climate. *Science*, v. 329, n. 5993, p.834-838, 2010.
- BREIMAN, L.; CUTLER, A.; LIAW, A. Package 'randomforest'. 2018. 29p. Available at: <https://cran.yu.ac.kr/web/packages/randomForest/randomForest.pdf>. Accessed in: September 18, 2018.
- CAPOLUPO, A.; SAPONARO, M.; FRATINO, U., *et al.* Detection of spatio-temporal changes of vegetation in coastal areas subjected to soil erosion issue. *Aquatic Ecosystem Health & Management*, v. 23, n. 4, p.491-499, 2020.
- CARRILLO-ANZURES, F.; ACOSTA-MIRELES, M.; FLORES-AYALA, E., *et al.* Caracterización de productores forestales en 12 estados de la República Mexicana. *Revista Mexicana De Ciencias Agrícolas*, v. 8, n. 7, p.1561-1573, 2017.
- CHANDER, G.; MARKHAM, B. L.; HELDER, D. L. Summary of current radiometric calibration coefficients for Landsat MSS, TM, ETM+, and EO-1 ALI sensors. *Remote Sensing of Environment*, v. 113, n. 5, p.893-903, 2009.
- CHÁVEZ-AGUILAR, G.; PÉREZ-SUÁREZ, M.; GAYOSSO-BARRAGÁN, O., *et al.* Forest management accelerates aboveground biomass accumulation in a temperate forest of Central Mexico. *Revista Chapingo Serie Ciencias Forestales y del Ambiente*, v. 29, n. 1, p.15-33, 2022.
- COMISIÓN NACIONAL FORESTAL [CONAFOR]. Manual y procedimientos para el muestreo de campo: Re-muestreo 2012. SEMARNAT: Zapopan, Jalisco, México, 2012.
- DUGAN, A. J.; BIRDSEY, R.; MASCORRO, V. S., *et al.* A systems approach to assess climate change mitigation options in landscapes of the United States forest sector. *Carbon Balance and Management*, v. 13, n. 1, p.14, 2018.
- FAO. Global Forest Resources Assessment 2020: Main report. Rome, Italy, 2020. 164p. Available at: <https://pipap.sprep.org/content/global-forest-resources-assessment-2020-main-report>. Accessed in: June 1, 2023.

- FREEMAN, E. A.; FRESCINO, T. S.; MOISEN, G. G. Package ModelMap: an R package for model creation and map production. 2018. 52p. Available at: <https://cran.r-project.org/web/packages/ModelMap/ModelMap.pdf>. Accessed in: September 18, 2018.
- GOSLEE, S. C. Analyzing Remote Sensing Data in R: The landsat Package. *Journal of Statistical Software*, v. 43, n. 4, p.1 - 25, 2011.
- HASTIE, T.; TIBSHIRANI, R. Generalized Additive Models. In *Encyclopedia of Statistical Sciences*.
- HERNÁNDEZ-STEFANONI, J. L.; CASTILLO-SANTIAGO, M. Á.; ANDRES-MAURICIO, J., et al. Mapeo de la biomasa aérea de los bosques mediante datos de sensores remotos y R. El Colegio de la Frontera Sur y Centro de Investigación Científica de Yucatán, A.C. 2021a. 128p.
- HERNÁNDEZ-STEFANONI, J. L.; CASTILLO-SANTIAGO, M. Á.; ANDRES-MAURICIO, J., et al. Carbon Stocks, Species Diversity and Their Spatial Relationships in the Yucatán Peninsula, Mexico. *Remote Sensing*, v. 13, n. 16, p.3179, 2021b.
- HERNÁNDEZ-STEFANONI, J. L.; CASTILLO-SANTIAGO, M. Á.; MAS, J. F., et al. Improving aboveground biomass maps of tropical dry forests by integrating LiDAR, ALOS PALSAR, climate and field data. *Carbon Balance and Management*, v. 15, n. 1, p.15, 2020.
- JIANG, X.; LI, G.; LU, D., et al. Stratification-Based Forest Aboveground Biomass Estimation in a Subtropical Region Using Airborne Lidar Data. *Remote Sensing*, v. 12, n. 7, 1101, 2020.
- KÖHL, M.; EHRHART, H.-P.; KNAUF, M., et al. A viable indicator approach for assessing sustainable forest management in terms of carbon emissions and removals. *Ecological Indicators*, v. 111, p.106057, 2020.
- LEUTNER, B.; HORNING, N.; LEUTNER, M. B. Package 'RStoolbox'. Version: 0.2.6; 2019.
- LI, C.; LI, Y.; LI, M. Improving Forest Aboveground Biomass (AGB) Estimation by Incorporating Crown Density and Using Landsat 8 OLI Images of a Subtropical Forest in Western Hunan in Central China. *Forests*, v. 10, n. 2, p.104, 2019.
- LI, Y.; LI, M.; LI, C., et al. Forest aboveground biomass estimation using Landsat 8 and Sentinel-1A data with machine learning algorithms. *Scientific Reports*, v. 10, n. 1, p.9952, 2020.
- LIAO, Z.; LIU, X.; VAN DIJK, A., et al. Continuous woody vegetation biomass estimation based on temporal modeling of Landsat data. *International Journal of Applied Earth Observation and Geoinformation*, v. 110, p.102811, 2022.
- LU, D.; CHEN, Q.; WANG, G., et al. A survey of remote sensing-based aboveground biomass estimation methods in forest ecosystems. *International Journal of Digital Earth*, v. 9, n. 1, p.63-105, 2016.
- MACEDO, F. L.; SOUSA, A. M. O.; GONÇALVES, A. C., et al. Above-ground biomass estimation for *Quercus rotundifolia* using vegetation indices derived from high spatial resolution satellite images. *European Journal of Remote Sensing*, v. 51, n. 1, p.932-944, 2018.
- MONÁRREZ-GONZÁLEZ, J. C.; PÉREZ-VERDÍN, G.; LÓPEZ-GONZÁLEZ, C., et al. Efecto del manejo forestal sobre algunos servicios ecosistémicos en los bosques templados de México. *Madera y bosques*, v. 24, n. 2, 2018.
- MORALES-BARQUERO, L.; SKUTSCH, M.; JARDEL-PELÁEZ, E. J., et al. Operationalizing the Definition of Forest Degradation for REDD+, with Application to Mexico. *Forests*, v. 5, n. 7, p.1653-1681, 2014.
- OCHOA-FRANCO, A. D. P.; VALDEZ-LAZALDE, J. R.; ÁNGELES-PÉREZ, G., et al. Beta-Diversity Modeling and Mapping with LiDAR and Multispectral Sensors in a Semi-Evergreen Tropical Forest. *Forests*, v. 10, n. 5, p.419, 2019.
- OLUSEGUN, A. M.; DIKKO, H. G.; GULUMBE, S. U. Identifying the limitation of stepwise selection for variable selection in regression analysis. *American Journal of Theoretical and Applied Statistics*, v. 4, n. 5, p.414-419, 2015.
- ORTIZ-REYES, A. D.; VALDEZ-LAZALDE, J. R.; ÁNGELES-PÉREZ, G., et al. Synergy of Landsat, climate and LiDAR data for aboveground biomass mapping in medium-stature tropical forests of the Yucatan Peninsula, Mexico. *Revista Chapingo Serie Ciencias Forestales*, v. 27, n. 3, 2021.
- ORTIZ-REYES, A. D.; VALDEZ-LAZALDE, J. R.; DE LOS SANTOS-POSADAS, H. M., et al. Inventario y cartografía de variables del bosque con datos derivados de LiDAR: comparación de métodos. *Madera y Bosques*, v. 21, n. 3, p.111-128, 2015.
- PÉREZ-LÓPEZ, R. I.; GONZÁLEZ-ESPINOSA, M.; RAMÍREZ-MARCIAL, N., et al. Efectos del "Método de Desarrollo Silvícola" sobre la diversidad arbórea en bosques húmedos de montaña del norte de Chiapas, México. *Revista Mexicana de Biodiversidad*, v. 91, n.91, 2020.
- RODRÍGUEZ-VEIGA, P.; SAATCHI, S.; TANSEY, K., et al. Magnitude, spatial distribution and uncertainty of forest biomass stocks in Mexico. *Remote Sensing of Environment*, v. 183, p.265-281, 2016.
- ROLDÁN-CORTÉS, M. A.; DE LOS SANTOS-POSADAS, H. M., et al. Estimadores de muestreo para inventario de plantaciones forestales comerciales de eucalipto en el sureste mexicano. *Revista Mexicana de Ciencias Forestales*, v. 5, n. 26, p.38-57, 2013.
- ROMERO-SANCHEZ, M. E.; PONCE-HERNANDEZ, R. Assessing and Monitoring Forest Degradation in a Deciduous Tropical Forest in Mexico via Remote Sensing Indicators. *Forests*, v. 8, n. 9, p.302, 2017.
- ROY, D. P.; WULDER, M. A.; LOVELAND, T. R., et al. Landsat-8: Science and product vision for terrestrial global change research. *Remote Sensing of Environment*, v. 145, p.154-172, 2014.
- SADER, S. A.; WAIDE, R. B.; LAWRENCE, W. T., et al. Tropical forest biomass and successional age class relationships to a vegetation index derived from landsat TM data. *Remote Sensing of Environment*, v. 28, p.143-198, 1989.
- SECRETARÍA DE MEDIO AMBIENTE Y RECURSOS NATURALES [SEMARNAT]. Anuario estadístico de la producción forestal 2018. Primera ed.; México, 2021; p 297.
- SERVICIO METEOROLÓGICO NACIONAL [SMN]. Normales climatológicas. 2020.
- SHE, X.; ZHANG, L.; CEN, Y., et al. Comparison of the Continuity of Vegetation Indices Derived from Landsat 8 OLI and Landsat 7 ETM+ Data among Different Vegetation Types. *Remote Sensing*, v. 7, n. 10, p.13485-13506, 2015.
- SILLEOS, N. G.; ALEXANDRIDIS, T. K.; GITAS, I. Z., et al. Vegetation Indices: Advances Made in Biomass Estimation and Vegetation Monitoring in the Last 30 Years. *Geocarto International*, v. 21, n. 4, p.21-28, 2006.
- SINGH, A.; KUSHWAHA, S. K. P.; NANDY, S., et al. Aboveground Forest Biomass Estimation by the Integration of TLS and ALOS PALSAR Data Using Machine Learning. *Remote Sensing*, v. 15, n. 4, p.1143, 2023.
- SORIANO-LUNA, M. D. L. Á.; ÁNGELES-PÉREZ, G.; GUEVARA, M., et al. Determinants of Above-Ground Biomass and Its Spatial Variability in a Temperate Forest Managed for Timber Production. *Forests*, v. 9, n. 8, p.490, 2018.
- SORIANO-LUNA, M. D. L. Á.; ÁNGELES-PÉREZ, G.; MARTÍNEZ-TRINIDAD, T., et al. Estimación de biomasa aérea por componente estructural en Zacualtipán, Hidalgo, México. *Agrociencia*, v. 49, n. 4, p.423-438, 2015.
- STEINHAUSEN, M. J.; WAGNER, P. D.; NARASIMHAN, B., et al. Combining Sentinel-1 and Sentinel-2 data for improved land use and land cover mapping of monsoon regions. *International Journal of Applied Earth Observation and Geoinformation*, v. 73, p.595-604, 2018.
- TORRES-ROJO, J. M.; MORENO-SÁNCHEZ, R.; MENDOZA-BRISEÑO, M. A. Sustainable Forest Management in Mexico. *Current Forestry Reports*, v. 2, n. 2, p.93-105, 2016.
- TORRES-VIVAR, J. E.; VALDEZ-LAZALDE, J. R.; ÁNGELES-PÉREZ, G., et al. Inventario y mapeo de un bosque bajo manejo de pino con datos del sensor SPOT 6. *Revista Mexicana de Ciencias Forestales*, v. 8, n. 39, p.25-44, 2017.
- TYRALIS, H.; PAPACHARALAMPOUS, G.; TANTANEE, S. How to explain and predict the shape parameter of the generalized extreme value distribution of streamflow extremes using a big dataset. *Journal of Hydrology*, v. 574, p.628-645, 2019.
- URBAZAEV, M.; THIEL, C.; MIGLIAVACCA, M., et al. Improved Multi-Sensor Satellite-Based Aboveground Biomass Estimation by Selecting Temporally Stable Forest Inventory Plots Using NDVI Time Series. *Forests*, v. 7, n. 8, p.169, 2016.
- VÁSQUEZ-GRANDÓN, A.; DONOSO, P. J.; GERDING, V. Forest Degradation: When Is a Forest Degraded? *Forests*, v. 9, n. 11, p.726, 2018.

WOOD, S.; WOOD, M. S. Package 'mgcv'. R Package Version, v. 1, n. 29, p.729, 2015.

WULDER, M. A.; MASEK, J. G.; COHEN, W. B., et al. Opening the archive: How free data has enabled the science and monitoring promise of Landsat. *Remote Sensing of Environment*, v. 122, n., p.2-10, 2012.

ZHANG, L.; CHENG, Q.; LI, C. Improved model for estimating the biomass of *Populus euphratica* forest using the integration of spectral and textural features from the Chinese high-resolution remote sensing satellite GaoFen-1. *Journal of Applied Remote Sensing*, v. 9, n. 1, p.096010, 2015.

ZHOU, H.; FU, L.; SHARMA, R. P., et al. A Hybrid Approach of Combining Random Forest with Texture Analysis and VDVl for Desert Vegetation Mapping Based on UAV RGB Data. *Remote Sensing*, v. 13, n. 10, p.1891, 2021.

ZHU, Z.; HUANG, M.; ZHOU, Z., et al. Stronger conservation promotes mangrove biomass accumulation: Insights from spatially explicit assessments using UAV and Landsat data. *Remote Sensing in Ecology and Conservation*, v. 8, n., 2022.

ZVOLEFF, A. Calculate Textures from Grey-Level Co-Occurrence Matrices (GLCMs); Package 'glcm'. Version: 1.6.5; Arlington, VA, USA, 2020.